HHS Public Access

Author manuscript

ACS Synth Biol. Author manuscript; available in PMC 2018 May 01.

Published in final edited form as:

ACS Synth Biol. 2018 April 20; 7(4): 1167–1173. doi:10.1021/acssynbio.7b00455.

Remote Control of Mammalian Cells with Heat-Triggered Gene Switches and Photothermal Pulse Trains

Ian C. Miller[†], **Marielena Gamboa Castro**[†], **Joe Maenza**[†], **Jason P. Weis**[†], and **Gabriel A. Kwong**[*,†,‡,§,||,⊥]

[†]The Wallace H. Coulter Department of Biomedical Engineering, Georgia Institute of Technology and Emory University, Atlanta, Georgia 30332, United States

[‡]Institute for Electronics and Nanotechnology, Georgia Institute of Technology, Atlanta, Georgia 30332, United States

[§]Parker H. Petit Institute of Bioengineering and Bioscience, Georgia Institute of Technology, Atlanta, Georgia 30332, United States

[||]Integrated Cancer Research Center, Georgia Institute of Technology, Atlanta, Georgia 30332, United States

[⊥]Georgia Immunoengineering Consortium, Emory University and Georgia Institute of Technology, Atlanta, Georgia 30332, United States

Abstract

Engineered T cells are transforming broad fields in biomedicine, yet our ability to control cellular activity at specific anatomical sites remains limited. Here we engineer thermal gene switches to allow spatial and remote control of transcriptional activity using pulses of heat. These gene switches are constructed from the heat shock protein HSP70B′ (HSPA6) promoter, show negligible basal transcriptional activity, and activate within an elevated temperature window of 40–45 °C. Using engineered Jurkat T cells implanted *in vivo*, we use plasmonic photothermal heating to trigger gene expression at specific sites to levels greater than 200-fold. We show that delivery of heat as thermal pulse trains significantly increase cellular thermal tolerance compared to continuous heating curves with identical area-under-the-curve (AUC), enabling long-term control of gene expression in Jurkat T cells. This approach expands the toolkit of remotely controlled genetic devices for basic and translational applications in synthetic immunology.

[*]Corresponding Author: Phone: 404-385-3746. gkwong@gatech.edu.

ORCID

Gabriel A. Kwong: 0000-0002-6255-6755

Author Contributions

I.C.M. and G.A.K. conceived of the idea. I.C.M., M.G.C. and G.A.K. designed the experiments and interpreted results. I.C.M., M.G.C., J.P.W. and J.M. performed the experiments. I.C.M. and G.A.K. wrote the manuscript.

Notes

The authors declare no competing financial interest.

Supporting Information

The Supporting Information is available free of charge on the ACS Publications website at DOI: 10.1021/acssynbio.7b00455. Basal activity of HSPA6 switch in Jurkat T cells; Heat actuation of engineered Jurkat T cells; Mild hyperthermia is well-tolerated by Jurkat T cells; Spatially selective activation of thermal switches; Supplementary Methods (PDF)

Graphical abstract

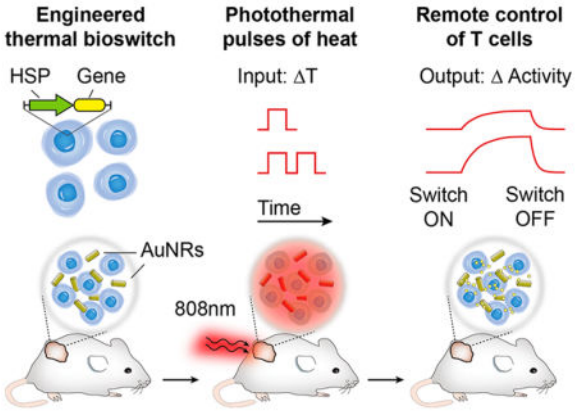

Keywords

engineered T cells; remote control; thermal gene switches; photothermal heating; plasmonic nanoparticles

Recent developments in mammalian synthetic biology are providing new approaches to control complex cellular activity, such as cell signaling, communication, and differentiation using orthogonal cues including small-molecules, proteins, or light.[1–3] These advances are leading to numerous applications for synthetic immunology; in particular, the design of engineered T cells with entirely new abilities[4] such as the capacity to migrate toward synthetic chemical cues,[5] deliver drugs to tumors,[6] employ logic-gates to sense antigens,[7] and target cancer with chimeric receptors.[8] Despite these advances, our ability to precisely control T cell gene expression at specific anatomical sites *in vivo* remains limited. This is particularly important for therapeutic applications of engineered T cells. Clinically used methods to control T cells that involve systemic administration of potent immune-modulating drugs[9] or biologics[10,11] lack spatial and temporal precision and can be associated with significant adverse effects.[12] Engineered T cells capable of being locally activated at desired locations in the body by externally applied cues—such as light[3,13] or radio waves[14]—will increase the precision of engineered T cell applications for use in humans.

Inspired by the precision with which pulses of heat can be delivered to sites located both superficially and at depth inside the body (*e.g.*, by laser heating,[15] induction heating,[16] or focused ultrasound[17]), we engineer Jurkat T cells with heat-triggered gene switches for remote control of transcriptional activity by plasmonic photothermal heating. Temperature control has a rich and longstanding clinical history such as the use of freezing temperatures for cryoablation[18] and hyperthermia to increase radiosensitivity[19] or enhance drug delivery.[20] Despite this, few engineered genetic systems have been designed that leverage temperature triggers to regulate cellular activity. Past work on mammalian gene switches include transcriptional activity triggered by small molecules, protein ligands, and light.[1] Genetically encoded thermal switches such as RNA thermometers[21] or temperature-sensitive

transcriptional regulators[22,23] have been developed for bacterial systems, but the prokaryotic origin of these approaches raises concerns with immunogenicity in T cells and potentially limits their use for cellular control in mammalian systems. By contrast, our thermal gene switches are constructed from endogenous promoters that drive the heat shock (HS) response, a highly conserved reactive mechanism to transient elevations in temperature (~3–5 °C above basal temperature) that triggers expression of protective HS proteins at levels comparable to the strongest known viral promoters.[24] The ubiquity of the HS response has driven past work on thermal gene regulatory systems in mammals, worms, fish and other organisms,[25] including the use of plasmonic nanomaterials to remotely activate engineered cells.[26–29] However, these approaches activated wild-type promoters with continuous heating methods that result in low cellular viability[30] and preclude their use for longitudinal control of cells.

Here we show that Jurkat T cells engineered with thermal gene switches constructed from the heat shock protein 70B′ (HSPA6) promoter have negligible activity at basal body temperatures but trigger gene expression to levels greater than 200-fold following exposure to elevated temperatures within a narrow transition window (40–42 °C). We spatially control Jurkat T cell activity with heat delivered by the photothermal effect using the precision of near-infrared (NIR) laser light for targeting and plasmonic gold nanorods as transducers to convert incident NIR light into localized heat.[15] We also demonstrate that the use of thermal pulse trains compared to heat delivered at a constant temperature significantly increases thermal tolerance to allow long-term control of Jurkat T cells for weeks in a living host.

RESULTS

Engineering a Thermal Gene Switch

Within the mammalian family of HS promoters, heat responsiveness is primarily mediated by Heat Shock Factor 1 (HSF1), a transcription factor that is normally present as an inactive monomer under basal conditions. During hyperthermia, HSF1 is converted to a homotrimer that then binds to heat shock response elements (HSEs) arrayed upstream of the transcription start site.[31,32] These HSEs, together with putative negative regulatory regions, dictate the heat response characteristics of a promoter. Therefore, we sought to perform truncation analysis on the HSPA6 locus to characterize different regions of the wild-type promoter sequence to identify constructs with low basal activity and high fold-induction.[33,34] We cloned 8 candidate constructs (labeled i–viii, Figure 1a) into HEK 293T cells starting at four upstream sites at −2964, −1231, −648, and −71 bp relative to the transcriptional start site, and ending at two downstream sites at +48 and +119 bp— the latter corresponding to the beginning of the open reading frame (ORF) of the HSPA6 gene. From our library, we selected construct ii for use in further studies based on several considerations: it had a high fold-induction, absolute level of activity, and small base pair footprint to allow larger gene inserts into viral vectors.

We next evaluated thermal switch activity in Jurkat T cells. While both transduced and untransduced cells did not produce measurable levels of Gluc luminescence at 37 °C (Figure S1), transduced Jurkat T cells incubated at 42 °C showed a sharp switch-on transition 6 h after heat treatment that resulted in a ~70-fold increase in luminescent signals (Figure 1b).

At time points greater than 9 h, no appreciable decrease in signals were observed that would indicate a switch-off transition. We attributed this result to the Gluc reporter we used because it is naturally secreted and not subject to intracellular degradation pathways such as ubiquitination. Therefore, to measure our thermal switch-off kinetics, we repeatedly sampled and replaced the cellular supernatant after maximum Gluc activity was attained at 9 h and determined a decay constant half-life of ~1h (Figure 1c). Additionally, incorporation of a GFP reporter revealed that ~90% of transduced Jurkats were actuated by heat treatments (Figure S2). These results show that thermal switches constructed from the HSPA6 promoter exhibit sharp switch-on and switch-off kinetics in transduced Jurkat T cells.

Triggering Cellular Activity with Pulses of Heat

To determine the relationship between heating duration, temperature, and thermal switch activity using continuous temperature inputs, we heated transduced Jurkat T cells for 15–60 min at temperatures ranging between 37 and 42 °C (Figure 2a,b). Elevations in temperature as low as 39 °C (ΔT = 2 °C) were sufficient to induce switch activity, and either higher temperatures or extended heating durations increased output activity, with maximal levels occurring at 41–42 °C. Moreover, our data showed that the level of thermal switch activity was independent of path; therefore, we hypothesized that milder heating conditions using discrete pulses of heat could be used to increase T cell thermal tolerance yet achieve similar levels of thermal switch activity.

To test this, we compared the efficacy of delivering heat using pulse train or constant temperature profiles (Figure 2c). Under a 67% duty cycle comprised of a 10 min heat step at 42 °C and 5 min rest period at 37 °C, each additional thermal pulse progressively increased cell output activity such that the cumulative effect from three pulses was ~50% higher compared to the intensity obtained using a constant temperature profile (*i.e.*, 100% duty cycle) with an identical area under the curve (AUC) (Figure 2d). We observed a similar trend where output activity increased with the number of pulses at a lower activating temperature of 40 °C; however, the level of activity between three pulses and continually heated samples was statistically identical. We attributed this difference between 40 and 42 °C to the ability of Jurkats to better tolerate smaller elevations in temperature. To test this, we analyzed Jurkat viability by Annexin V and propidium iodide (PI) stains for apoptosis and cell death respectively, and found that at 42 °C, a 67% duty cycle significantly reduced double positive cells by over 70% compared to continuous heating, and maintained a cell viability of ~90% relative to that of unheated cells (Figure 2e,f). Conversely, no significant differences in cell death and viability were observed at 40 °C even after 40 min of constant heating (Figure S3). Collectively, our data showed that the number of pulses in a thermal train controls the level of output activity and significantly increases thermal tolerance of Jurkat T cells compared to constant temperature inputs.

Photothermal Targeting of Jurkat T Cells

We next set out to demonstrate temperature control of Jurkat T cells using externally applied triggers. Spatially targeted heating in human patients can be achieved in deep tissues using multiple platforms including focused ultrasound, inductive heating, and microwave heating.[20] Here we chose photothermal heating using near-infrared (NIR) laser light (λ = 808 nm)

irradiation of plasmonic gold nanorods (AuNRs).[15] AuNRs are long-circulating nanomaterials whose geometry can be precisely tuned to absorb and convert incident NIR light into thermal energy by surface plasmon resonance (SPR) (Figure 3a). Passively targeted AuNRs accumulate in tissue across fenestrated endothelium such as tumors[35,36] and allow for localized heating when the site is exposed to otherwise benign NIR light. To test this approach, we arrayed mixtures of AuNRs and luciferized Jurkats into a 96-well plate and confirmed coincident increases in both temperature and luciferase activity in wells treated with NIR laser light (Figure 3b), allowing spatial targeting of cellular expression in patterns such as the Georgia Tech logo (Figure S4). We then tested this system *in vivo* by laser heating subcutaneous matrigel implants encapsulated with Jurkat T cells and AuNRs (Figure 3c) under the guidance of a thermal camera to allow maintenance of target skin temperatures in real time (Figure 3d,e). At implant sites heated to focal skin surface temperatures of 42 and 45 °C, we observed over 105-fold and 209-fold increases in luciferase activity respectively compared to unheated sites kept at body temperature (Figure 3f). In contrast to our *in vitro* studies showing maximum cell activation at 42 °C (Figure 2b), a surface skin temperature of 45 °C was required to robustly trigger our thermal switch *in vivo*. We attributed this difference to measuring temperature at the surface of the skin compared to the core of the implant. We did not observe tissue damage to the skin surface at 45 °C and chose to work with this activating temperature for further *in vivo* studies. Taken together, our data showed that photothermal heating using NIR light and AuNRs effectively allows spatial targeting and control of cellular activity *in vivo.*

Thermal Pulse Trains for Long-Term Control of Jurkat T Cells *In Vivo*

On the basis of our *in vitro* studies which showed the benefits of heat delivery using thermal pulse trains, we sought to determine whether this method could be used to control Jurkat T cells over several weeks without significant reductions in cell viability and function. Serial modulation of T cell phenotype is especially relevant to chronic diseases such as HIV or refractory cancer that produce exhausted or anergic T cell populations[37] and where recovering T cell effector functions requires repeated administration of activating drugs (*e.g.*, cytokines and checkpoint blockade antibodies). To enable localized, extended control over Jurkat T cell behavior while maintaining high cell viability, we applied thermal pulse trains to repeatedly heat matrigel implant sites serially using NIR laser light and AuNRs. To confirm that the rate of heat transfer *in vivo* would allow on–off cycling of thermal pulses, we irradiated implant sites at a 67% duty cycle which produced discrete skin temperature profiles characterized by a decay half-life of 1.7 min between pulses and an area under the curve (AUC) of 1.2 compared to the ideal square wave input (Figure 4a). We then compared the viability of Jurkats recovered from *in vivo* matrigel implants heated with thermal pulse trains to those treated by continuous heating (Figure 4b) and, consistent with *in vitro* studies (Figure 2e,f), found greater than a 70% increase in viability (Annexin V^-, PI^-) within pulsed cells after 1 day (Figure 4c). Because of this significant reduction in viability using a constant temperature profile, we explored long-term control of cell behavior using repeated pulsatile heat treatments. Over the course of 14 days, implanted Jurkats steadily increased switch activity compared to unheated controls such that signals by Day 14 were more than 4-fold higher than on Day 1 (Figure 4d,e). To confirm long-term pulsatile heating did not adversely affect implanted cells, we analyzed the Jurkat T cells on Day 15 and observed no

significant differences in apoptosis and cell death markers (Annexin V and PI) between pulsed and unheated cells kept at body temperature that were implanted concomitantly on Day 0 (Figure 4f). Together our data shows that heat delivered in discrete pulses preserves cell viability and allows remote control of Jurkat T cells for weeks *in vivo*.

DISCUSSION

Inspired by remote control of biological systems, we establish a framework for engineering mammalian cells with thermal gene switches for *in vivo* control using pulses of heat. Thermal gene switches constructed from the HSPA6 promoter activate within a narrow temperature window of 40–42 °C and trigger gene expression to hundreds of fold above basal levels while remaining silent at normal body temperature. Here we used wild-type promoter sequences but key thermal switch properties, including thermal activation temperatures and on–off ratios, could be further developed by directed evolution or incorporating similar genetic architectures from a wide range of species that have different temperature thresholds for heat shock activation (*e.g.*, Arabian camel and zebrafish). This could provide orthogonal thermal band-pass circuits that express different genes depending on the temperature of the hyperthermic input as demonstrated recently in bacteria.[23]

In our study, we found that pulsatile heat delivery significantly improved thermal tolerance of Jurkat T cells compared to continuous heating profiles with identical AUCs, which allowed long-term control of cells *in vivo* without reduction in output activity or cellular viability. In past studies, thermal tolerance was achieved by pretreatment of cells with mild heat followed by a rest period to allow expression of protective HSPs before full thermal induction;[38] however, this mechanism is unlikely to explain our results as our off-cycle interval (~5 min) did not allow sufficient time for protein expression. The induction of thermal tolerance under our heating schedule may be related to HSF1's trimerization mechanism in which hydrophobic regions in repeated heptad domains are disrupted and form intermolecular coiled coils in response to hyperthermic conditions. These interactions allow HSF1 to stably trimerize and bind with high affinity to HSEs to initiate transcription.[24,31,32] Our pulsed delivery method may influence the rate at which these hydrophobic domains are exposed, or the population frequency of trimers since higher-order oligomers are formed as well.[39,40] The exact mechanism may be elucidated by examining the heat-response of substitution or deletion mutations within the hydrophobic domains that govern and regulate HSF1 trimerization.[39,41–44]

To heat specific sites *in vivo*, we chose to use NIR laser light and plasmonic gold nanorods to induce local hyperthermia in matrigel implants. The well-established biodistribution of nanoparticles[45] in tissues with porous vessels such as secondary lymphoid organs (*e.g.*, spleen or lymph nodes) or sites of disease (*e.g.*, tumors) could allow engineered cells within these tissues to be remotely controlled. In humans, modalities such as focused ultrasound, radio- or microwaves are routinely used to precisely heat deeper tissues where targeting with optical techniques remains challenging.[20] In a clinical setting, a future application is to incorporate thermal gene switches into engineered T cell therapies for cancer to allow local expression of potent immune-modulating biologics[10,11]—which are otherwise associated with significant off-target toxicity when administered systemically—to combat tumor

immunosuppression. Moreover, local heating may be targeted to sites implanted with biomaterials designed to enhance T cell function, including wafers that expand and disperse tumor-reactive T cells.[46] Looking forward, this framework of activating gene expression by heat provides an orthogonal mechanism to control cellular activity in addition to small-molecule[47] or light-based methods.[13] Such platforms may be integrated across different immune cell types for remote control of synthetic immunological systems.

METHODS

Plasmid Construction and Viral Production

The promoter of the HSPA6 gene (Uniprot P17066) was amplified from human genomic DNA (Clontech #636401) at positions indicated in Figure 1a similar to previous studies.[33] XbaI and XhoI sites were added to the 5′ and 3′ ends of annealing sequences listed in the Supplementary Methods, digested, and used to insert the promoters into the Lego-C plasmid (Addgene #27348) that contains the reporter mCherry as a selectable marker. This fluorescent reporter was used to sort transduced cells using FACS. Additional reporters including Gluc (LifeTech 16146), emGFP (Imanis DNA1023) and Fluc (Addgene #33307) were added under control of the heat shock promoter *via* restriction enzyme digestion and ligation. Plasmid DNA was purified using a Plasmid Maxi Kit (Qiagen cat #12163) and packaged into lentiviral vectors with psPAX2 (Addgene #12260) and pMD2.G (Addgene #12259). Cells were transduced in 10 μg/mL of protamine sulfate (Sigma) before FACS (BD FACS Aria) and downstream use.

Preparation of AuNRs

AuNRs were purchased from Nanopartz (item #A12-10-808-CTAB-500) and pegylated (Laysam Bio cat #MPEG-SH-5000-5g) to replace the CTAB coating before being resuspended in DI at 0.5 mg/mL. This solution was used in a 1:100 dilution for all laser-mediated heating experiments in mice and 96-well plates.

Viability Studies

Jurkats were heated in a thermal cycler (Biorad) in HEPES buffered RPMI (25 mM) at a density of 10^6 cells/mL and incubated at 37 °C and 5% CO_2. After 24 h, cells were assayed for viability using the Apoptosis Detection Kit (BD cat #556547). For cells recovered from implant sites, matrigel was excised from mice, physically dissociated and incubated in Cell Recovery Solution (Corning) according to manufacturer's instructions before analysis with Apoptosis Detection Kit 24 h after conclusion of heating. All samples were analyzed with FlowJo, Version 10 (FlowJo LLC).

In Vitro Heating Assays

Cells were heated in a thermal cycler and immediately transferred to a 96-well plate and incubated until assayed. Unless otherwise indicated, cellular supernatant was sampled for reporter activity 24 h after heating. Density inside PCR tubes was 10^6 cells/mL. Luminescent activity was measured using a Cytation 5 plate reader (BioTek) and Gaussia Luciferase Assay Kit (New England Biolabs) according to manufacturer's instructions.

In Vivo Laser Heating

0.5 μg AuNRs and 2×10^6 engineered cells per 100 μL matrigel were used for laser heating with *in vivo* implants after subcutaneous injection into in nude mice (Jackson Laboratories). Mice were anesthetized with isoflurane gas and implant sites were heated using an 808 nm laser (Coherent) at a power density of ~9.5 A/cm^2. All *in vivo* pulsatile heating profiles were performed for a total of 30 min of heat with a 67% duty cycle. Surface temperature was continually measured using a thermal camera (FLIR model 450sc). Rest periods during cyclic heating began when measured skin temperature reached 37 ± 1 °C.

In Vivo Bioluminescence and Imaging

Fluc activity was measured using an IVIS Spectrum CT (PerkinElmer) after i.p. injections of luciferin (Gold Bio) administered 4.5 h after conclusion of activating heat shock. Integration time was set to automatic and imaging was conducted for up to 1.5 h after injection. ROIs were defined within the Living Image software package (PerkinElmer) and measured as average radiance (photons s^{-1} cm^{-1} sr^{-1}).

Statistical Analysis

All results are presented as mean, and error bars show SEM. Statistical analysis was performed using statistical software (GraphPad Prism 6; GraphPad Software). *$p < 0.05$, **$p < 0.01$, ****$P < 0.0001$.

Supplementary Material

Refer to Web version on PubMed Central for supplementary material.

Acknowledgments

We thank Dr. A. F. Bagley (M.D. Anderson), Dr. J. E. Dahlman (Georgia Tech), Dr. H. T. Kissick (Emory), and Dr. K. R. Stevens (University of Washington) for their helpful insights during planning and experiments. This work was funded by the NIH Director's New Innovator Award (DP2HD091793), the National Center for Advancing Translational Sciences (UL1TR000454), and the Shurl and Kay Curci Foundation. I.C.M. is supported by the Georgia Tech TI:GER program. M.G.C. is supported by the National Institutes of Health GT BioMAT Training Grant under Award Number 5T32EB006343 and the National Science Foundation Graduate Research Fellowship under Grant No. DGE-1451512. G.A.K. holds a Career Award at the Scientific Interface from the Burroughs Wellcome Fund. This work was performed in part at the Georgia Tech Institute for Electronics and Nanotechnology, a member of the National Nanotechnology Coordinated Infrastructure, which is supported by the National Science Foundation (Grant ECCS-1542174). This content is solely the responsibility of the authors and does not necessarily represent the official views of the National Institutes of Health.

References

1. Auslander S, Fussenegger M. From gene switches to mammalian designer cells: present and future prospects. Trends Biotechnol. 2013; 31:155–168. [PubMed: 23245728]
2. Lienert F, Lohmueller JJ, Garg A, Silver PA. Synthetic biology in mammalian cells: next generation research tools and therapeutics. Nat Rev Mol Cell Biol. 2014; 15:95–107. [PubMed: 24434884]
3. Fenno L, Yizhar O, Deisseroth K. The Development and Application of Optogenetics. Annu Rev Neurosci. 2011; 34:389–412. [PubMed: 21692661]
4. Swartz MA, Hirosue S, Hubbell JA. Engineering approaches to immunotherapy. Sci Transl Med. 2012; 4:148rv149.

5. Park JS, Rhau B, Hermann A, McNally KA, Zhou C, Gong D, Weiner OD, Conklin BR, Onuffer J, Lim WA. Synthetic control of mammalian-cell motility by engineering chemotaxis to an orthogonal bioinert chemical signal. Proc Natl Acad Sci U S A. 2014; 111:5896–5901. [PubMed: 24711398]
6. Huang B, Abraham WD, Zheng Y, Bustamante Lopez SC, Luo SS, Irvine DJ. Active targeting of chemotherapy to disseminated tumors using nanoparticle-carrying T cells. Sci Transl Med. 2015; 7:291ra294.
7. Roybal KT, Rupp LJ, Morsut L, Walker WJ, McNally KA, Park JS, Lim WA. Precision Tumor Recognition by T Cells With Combinatorial Antigen-Sensing Circuits. Cell. 2016; 164:770–779. [PubMed: 26830879]
8. Jackson HJ, Rafiq S, Brentjens RJ. Driving CAR T-cells forward. Nat Rev Clin Oncol. 2016; 13:370–383. [PubMed: 27000958]
9. Murphy AG, Zheng L. Small molecule drugs with immunomodulatory effects in cancer. Hum Vaccines Immunother. 2015; 11:2463–2468.
10. Baumeister SH, Freeman GJ, Dranoff G, Sharpe AH. Coinhibitory Pathways in Immunotherapy for Cancer. Annu Rev Immunol. 2016; 34:539–573. [PubMed: 26927206]
11. Waldmann TA. The biology of interleukin-2 and interleukin-15: implications for cancer therapy and vaccine design. Nat Rev Immunol. 2006; 6:595–601. [PubMed: 16868550]
12. Kaehler KC, Piel S, Livingstone E, Schilling B, Hauschild A, Schadendorf D. Update on immunologic therapy with anti-CTLA-4 antibodies in melanoma: identification of clinical and biological response patterns, immune-related adverse events, and their management. Semin Oncol. 2010; 37:485–498. [PubMed: 21074064]
13. Tan P, He L, Han G, Zhou Y. Optogenetic Immunomodulation: Shedding Light on Antitumor Immunity. Trends Biotechnol. 2017; 35:215–226. [PubMed: 27692897]
14. Fagnoni FF, Zerbini A, Pelosi G, Missale G. Combination of radiofrequency ablation and immunotherapy. Front Biosci, Landmark Ed. 2008; 13:369–381.
15. Jain PK, Lee KS, El-Sayed IH, El-Sayed MA. Calculated absorption and scattering properties of gold nanoparticles of different size, shape, and composition: applications in biological imaging and biomedicine. J Phys Chem B. 2006; 110:7238–7248. [PubMed: 16599493]
16. Lubner MG, Brace CL, Hinshaw JL, Lee FT Jr. Microwave tumor ablation: mechanism of action, clinical results, and devices. J Vasc Interv Radiol. 2010; 21:S192–203. [PubMed: 20656229]
17. Haar GT, Coussios C. High intensity focused ultrasound: physical principles and devices. Int J Hyperthermia. 2007; 23:89–104. [PubMed: 17578335]
18. Sabel MS. Cryo-immunology: a review of the literature and proposed mechanisms for stimulatory versus suppressive immune responses. Cryobiology. 2009; 58:1–11. [PubMed: 19007768]
19. Wust P, Hildebrandt B, Sreenivasa G, Rau B, Gellermann J, Riess H, Felix R, Schlag PM. Hyperthermia in combined treatment of cancer. Lancet Oncol. 2002; 3:487–497. [PubMed: 12147435]
20. Chu KF, Dupuy DE. Thermal ablation of tumours: biological mechanisms and advances in therapy. Nat Rev Cancer. 2014; 14:199–208. [PubMed: 24561446]
21. Kortmann J, Narberhaus F. Bacterial RNA thermometers: molecular zippers and switches. Nat Rev Microbiol. 2012; 10:255–265. [PubMed: 22421878]
22. Gardner TS, Cantor CR, Collins JJ. Construction of a genetic toggle switch in Escherichia coli. Nature. 2000; 403:339–342. [PubMed: 10659857]
23. Piraner DI, Abedi MH, Moser BA, Lee-Gosselin A, Shapiro MG. Tunable thermal bioswitches for in vivo control of microbial therapeutics. Nat Chem Biol. 2017; 13:75–80. [PubMed: 27842069]
24. Lindquist S. The heat-shock response. Annu Rev Biochem. 1986; 55:1151–1191. [PubMed: 2427013]
25. Feder ME, Hofmann GE. Heat-shock proteins, molecular chaperones, and the stress response: evolutionary and ecological physiology. Annu Rev Physiol. 1999; 61:243–282. [PubMed: 10099689]
26. Miyako E, Deguchi T, Nakajima Y, Yudasaka M, Hagihara Y, Horie M, Shichiri M, Higuchi Y, Yamashita F, Hashida M, Shigeri Y, Yoshida Y, Iijima S. Photothermic regulation of gene expression triggered by laser-induced carbon nanohorns. Proc Natl Acad Sci U S A. 2012; 109:7523–7528. [PubMed: 22529368]

27. Deguchi T, Itoh M, Urawa H, Matsumoto T, Nakayama S, Kawasaki T, Kitano T, Oda S, Mitani H, Takahashi T, Todo T, Sato J, Okada K, Hatta K, Yuba S, Kamei Y. Infrared laser-mediated local gene induction in medaka, zebrafish and Arabidopsis thaliana. Dev, Growth Differ. 2009; 51:769–775. [PubMed: 19843153]
28. Ramos DM, Kamal F, Wimmer EA, Cartwright AN, Monteiro A. Temporal and spatial control of transgene expression using laser induction of the hsp70 promoter. BMC Dev Biol. 2006; 6:55. [PubMed: 17116248]
29. Andersson HA, Kim YS, O'Neill BE, Shi ZZ, Serda RE. HSP70 promoter-driven activation of gene expression for immunotherapy using gold nanorods and near infrared light. Vaccines (Basel, Switz). 2014; 2:216–227.
30. Jaque D, Martinez Maestro L, del Rosal B, Haro-Gonzalez P, Benayas A, Plaza JL, Martin Rodriguez E, Garcia Sole J. Nanoparticles for photothermal therapies. Nanoscale. 2014; 6:9494–9530. [PubMed: 25030381]
31. Akerfelt M, Morimoto RI, Sistonen L. Heat shock factors: integrators of cell stress, development and lifespan. Nat Rev Mol Cell Biol. 2010; 11:545–555. [PubMed: 20628411]
32. Richter K, Haslbeck M, Buchner J. The heat shock response: life on the verge of death. Mol Cell. 2010; 40:253–266. [PubMed: 20965420]
33. Ramirez VP, Stamatis M, Shmukler A, Aneskievich BJ. Basal and stress-inducible expression of HSPA6 in human keratinocytes is regulated by negative and positive promoter regions. Cell Stress Chaperones. 2015; 20:95–107. [PubMed: 25073946]
34. Hamajima F, Hasegawa T, Nakashima I, Isobe K. Genomic cloning and promoter analysis of the GAHSP40 gene. J Cell Biochem. 2002; 84:401–407. [PubMed: 11787069]
35. von Maltzahn G, Park JH, Lin KY, Singh N, Schwoppe C, Mesters R, Berdel WE, Ruoslahti E, Sailor MJ, Bhatia SN. Nanoparticles that communicate in vivo to amplify tumour targeting. Nat Mater. 2011; 10:545–552. [PubMed: 21685903]
36. von Maltzahn G, Park JH, Agrawal A, Bandaru NK, Das SK, Sailor MJ, Bhatia SN. Computationally guided photothermal tumor therapy using long-circulating gold nanorod antennas. Cancer Res. 2009; 69:3892–3900. [PubMed: 19366797]
37. Kim PS, Ahmed R. Features of responding T cells in cancer and chronic infection. Curr Opin Immunol. 2010; 22:223–230. [PubMed: 20207527]
38. Kregel KC. Heat shock proteins: modifying factors in physiological stress responses and acquired thermotolerance. J Appl Physiol. 2002; 92:2177–2186. [PubMed: 11960972]
39. Rabindran SK, Haroun RI, Clos J, Wisniewski J, Wu C. Regulation of heat shock factor trimer formation: role of a conserved leucine zipper. Science. 1993; 259:230–234. [PubMed: 8421783]
40. Clos J, Westwood JT, Becker PB, Wilson S, Lambert K, Wu C. Molecular cloning and expression of a hexameric Drosophila heat shock factor subject to negative regulation. Cell. 1990; 63:1085–1097. [PubMed: 2257625]
41. Hentze N, Le Breton L, Wiesner J, Kempf G, Mayer MP. Molecular mechanism of thermosensory function of human heat shock transcription factor Hsf1. eLife. 2016; doi: 10.7554/eLife.11576
42. Hensen SM, Heldens L, van Genesen ST, Pruijn GJ, Lubsen NH. A delayed antioxidant response in heat-stressed cells expressing a non-DNA binding HSF1 mutant. Cell Stress Chaperones. 2013; 18:455–473. [PubMed: 23321918]
43. Heldens L, Dirks RP, Hensen SM, Onnekink C, van Genesen ST, Rustenburg F, Lubsen NH. Co-chaperones are limiting in a depleted chaperone network. Cell Mol Life Sci. 2010; 67:4035–4048. [PubMed: 20556630]
44. Neef DW, Jaeger AM, Thiele DJ. Genetic selection for constitutively trimerized human HSF1 mutants identifies a role for coiled-coil motifs in DNA binding. G3: Genes, Genomes, Genet. 2013; 3:1315–1324.
45. Khlebtsov N, Dykman L. Biodistribution and toxicity of engineered gold nanoparticles: a review of in vitro and in vivo studies. Chem Soc Rev. 2011; 40:1647–1671. [PubMed: 21082078]
46. Stephan SB, Taber AM, Jileaeva I, Pegues EP, Sentman CL, Stephan MT. Biopolymer implants enhance the efficacy of adoptive T-cell therapy. Nat Biotechnol. 2015; 33:97–U277. [PubMed: 25503382]

47. Jensen MC, Riddell SR. Designing chimeric antigen receptors to effectively and safely target tumors. Curr Opin Immunol. 2015; 33:9–15. [PubMed: 25621840]

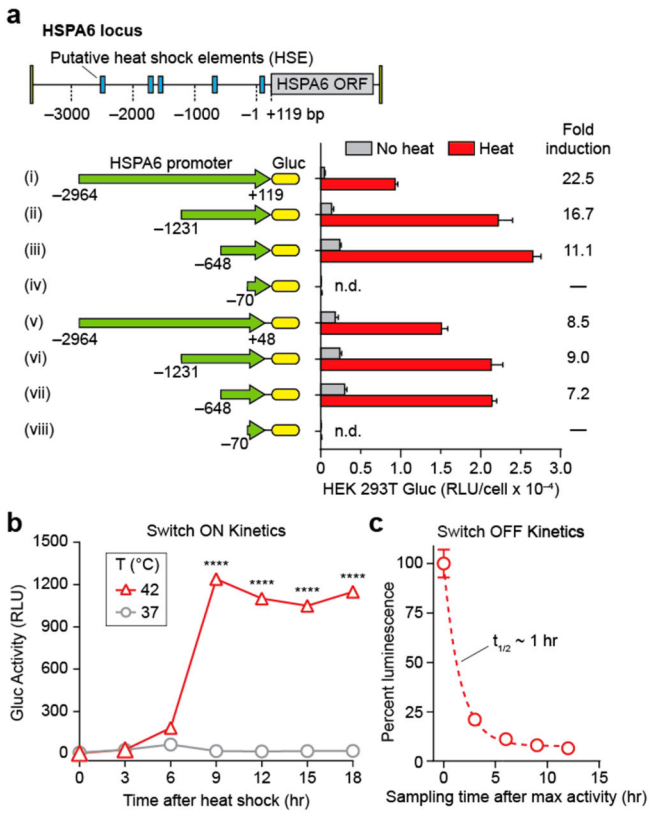

Figure 1.

Heat-triggered gene switches in Jurkat T cells. (a) Eight constructs (i–viii) cloned from the heat shock protein HSPA6 locus used to evaluate sensitivity to thermal activation in HEK 293T cells. Constructs i–iv extend to +119 bp beyond transcriptional start site while constructs v–viii terminate at +48 bp. Fold inductions of normalized luminescence (Heat/No heat) are listed to the right of each construct. RLU: Relative Luminescence Units, $n = 3$, error bars = SEM. (b) Kinetic trace of cumulative switch activity at 42 °C in Jurkat T cells following 1 h heating, $n = 3$, error bars show SEM and are smaller than the displayed data points, ****$P < 0.0001$, one-way ANOVA and Dunnett's multiple comparison test. (c) Decay kinetics of switch activation after 1 h heating at 42 °C. Luminescent values were determined by sampling and replacing supernatant after maximum activity was reached, $n = 3$, error bars = SEM.

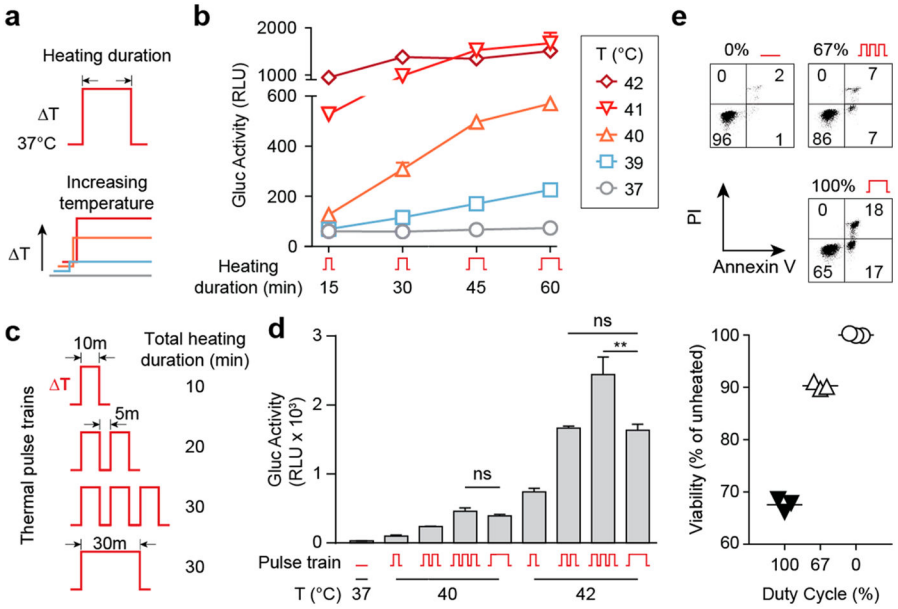

Figure 2.

Thermal pulse trains augment switch activity and enhance Jurkat thermal tolerance. (a) Continuous heat treatment profiles with increasing time or temperature. (b) Luminescent traces showing that increases in both duration and temperature of heating augment switch activity in a pathway-independent fashion, $n = 3$, error bars = SEM. (c) Diagram of thermal pulse trains at a 67% duty cycle (10 min on, 5 min off) and continuous heat treatments. Total heated time for last two regimens were identical (30 min). (d) Supernatant luminescence after discrete pulses (1, 2, or 3 cycles) or continuous heating at 40 and 42 °C, $n = 3$, $^{**}P < 0.01$, one-way ANOVA and Tukey's multiple comparison test, error bars = SEM (e) Propidium Iodide (PI) and Annexin V stains of Jurkat T cells heated at 42 °C. (f) Quantification of Jurkat viability across replicate samples and duty cycles. Total heating time = 30 min, $n = 3$.

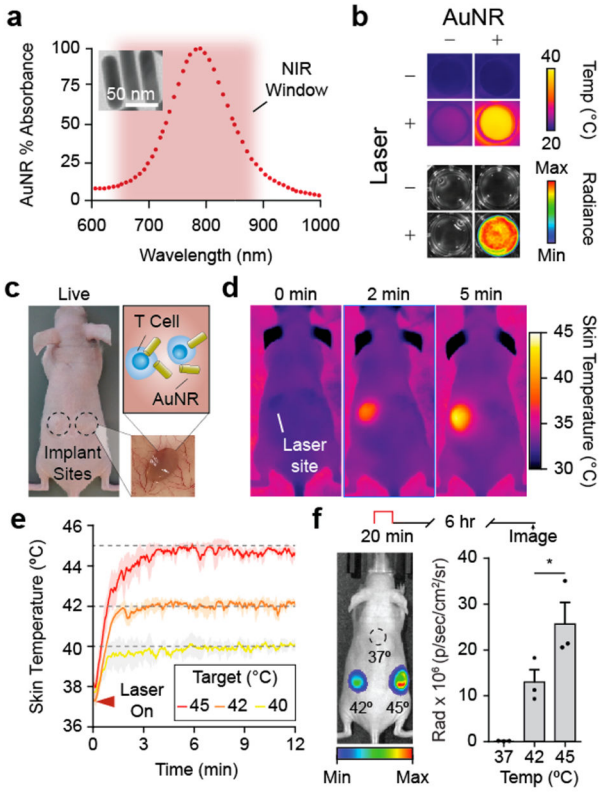

Figure 3.

Photothermal control of mammalian cells *in vivo*. (a) Absorbance spectrum of AuNRs with a with a maximum absorbance (805 nm) within the NIR window (~650–900 nm). (b) Top: thermograph of 96-well plate with wells containing engineered Jurkats with (+) and without (−) AuNRs and heated with NIR laser light (+) or unheated (−). Bottom: Luminescent image showing Fluc activity of engineered Jurkats contained only to wells with AuNRs (+) and heated with laser light (+) for 20 min at 42 °C. (c) Photograph of nude mouse with subcutaneous matrigel implants (inset) containing engineered Jurkat T cells and AuNRs before heating. (d) Serial thermal images of mouse bearing AuNR-matrigel implants within 5 min after laser activation. (e) Kinetic thermal traces (colored lines) showing average skin temperature of 3 × 3 pixel ROI centered on implant site immediately after laser is activated (triangle). Shaded regions around trace averages show STD of all heating runs, $n = 3$. (f) Radiant image of nude mouse with Jurkat implants after heating at skin temperatures of 37, 42, and 45 °C for 20 min. Radiance calculated as the difference in value between implant site luminescence and background radiance of mouse skin, $n = 3$, error bars = SEM.

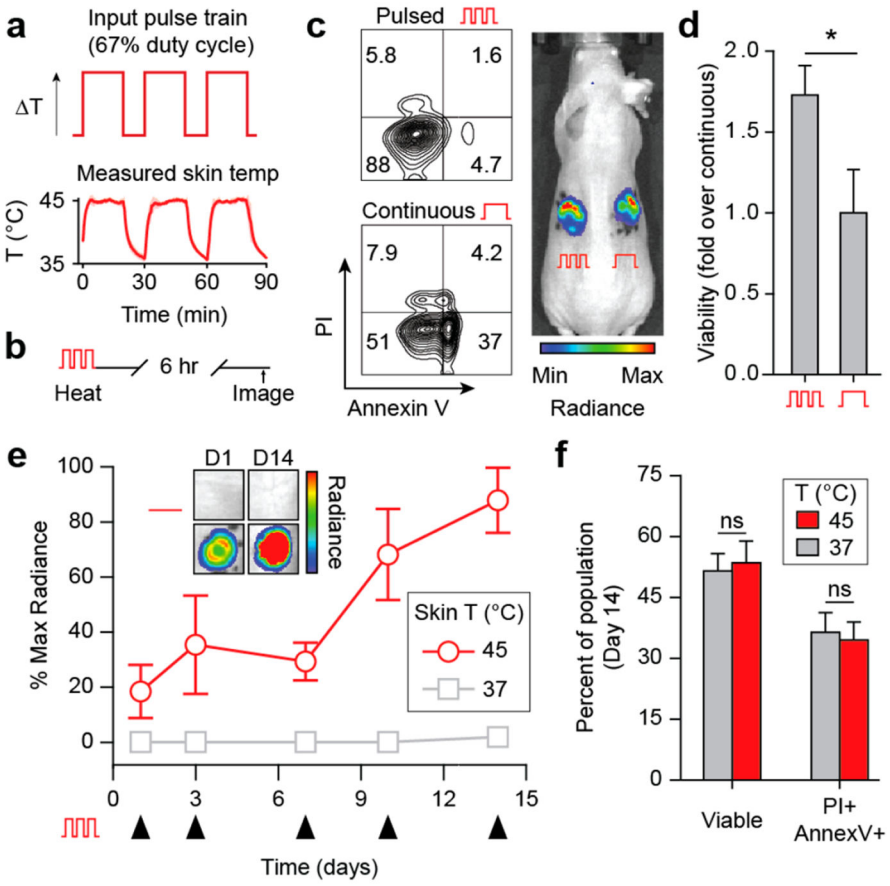

Figure 4.

In vivo pulsatile heating enables long-term control of mammalian cell activity. (a) Idealized pulse-wave thermal input with a 67% duty cycle (top) and trace of murine skin during photothermal treatment (bottom). Red line trace = average temperature of 3 × 3 pixel ROI centered on implant site during heating. Shaded regions around average trace show STD of three heating series, $n = 3$. (b) PI and Annexin V viability flow plots of Jurkats harvested from pulsatile and continuously heated implants, with (c) quantification, $n = 5–6$, error bars = SEM. (d) Radiance trace of implant sites after pulsatile heat treatments on days 1, 3, 7, 10, and 14 after implantation, $n = 4$, error bars = SEM. Inset: luminescent images of representative implant sites on days 1 and 14. (e) PI and Annexin V viability staining of Jurkats recovered from 37 and 45 °C heated implants in (d), $n = 3$, error bars = SEM, $*P < 0.05$, two-tailed *t* test.